Impact of climate change on renewable groundwater resources: assessing the benefits of avoided greenhouse gas emissions using selected CMIP5 climate projections



2013 Environ. Res. Lett. 8 024023

(http://iopscience.iop.org/1748-9326/8/2/024023)

OPEN ACCESS
IOP PUBLISHING ENVIRONMENTAL RESEARCH LETTERS
Environ. Res. Lett. **8** (2013) 024023 (14pp) doi:10.1088/1748-9326/8/2/024023

# Impact of climate change on renewable groundwater resources: assessing the benefits of avoided greenhouse gas emissions using selected CMIP5 climate projections

**Felix T Portmann[1,2,3], Petra Döll[1,3], Stephanie Eisner[4] and Martina Flörke[4]**

[1] Biodiversity and Climate Research Centre (LOEWE BiK-F), Senckenberganlage 25, D-60325 Frankfurt am Main, Germany
[2] Senckenberg Research Institute and Natural History Museum, Senckenberganlage 25, D-60325 Frankfurt am Main, Germany
[3] Institute of Physical Geography, Goethe University Frankfurt, Altenhöferallee 1, D-60438 Frankfurt am Main, Germany
[4] Center for Environmental Systems Research, University of Kassel, Wilhelmshöher Allee 47, D-34109 Kassel, Germany

E-mail: portmann@em.uni-frankfurt.de

Received 30 January 2013
Accepted for publication 1 May 2013
Published 15 May 2013
Online at stacks.iop.org/ERL/8/024023

**Abstract**
Reduction of greenhouse gas (GHG) emissions to minimize climate change requires very significant societal effort. To motivate this effort, it is important to clarify the benefits of avoided emissions. To this end, we analysed the impact of four emissions scenarios on future renewable groundwater resources, which range from 1600 $GtCO_2$ during the 21st century (RCP2.6) to 7300 $GtCO_2$ (RCP8.5). Climate modelling uncertainty was taken into account by applying the bias-corrected output of a small ensemble of five CMIP5 global climate models (GCM) as provided by the ISI-MIP effort to the global hydrological model WaterGAP. Despite significant climate model uncertainty, the benefits of avoided emissions with respect to renewable groundwater resources (i.e. groundwater recharge (GWR)) are obvious. The percentage of projected global population (SSP2 population scenario) suffering from a significant decrease of GWR of more than 10% by the 2080s as compared to 1971–2000 decreases from 38% (GCM range 27–50%) for RCP8.5 to 24% (11–39%) for RCP2.6. The population fraction that is spared from any significant GWR change would increase from 29% to 47% if emissions were restricted to RCP2.6. Increases of GWR are more likely to occur in areas with below average population density, while GWR decreases of more than 30% affect especially (semi)arid regions, across all GCMs. Considering change of renewable groundwater resources as a function of mean global temperature (GMT) rise, the land area that is affected by GWR decreases of more than 30% and 70% increases linearly with global warming from 0 to 3 °C. For each degree of GMT rise, an additional 4% of the global land area (except

Greenland and Antarctica) is affected by a GWR decrease of more than 30%, and an additional 1% is affected by a decrease of more than 70%.

**Keywords:** climate change, groundwater recharge, emissions scenarios, CMIP5 climate scenarios

## 1. Introduction

Groundwater is the source of ∼35% of global human water withdrawals, and even of ∼42% of global irrigation water withdrawals (Döll *et al* 2012, Siebert *et al* 2010). It is a more reliable and safer water source than surface water, because its use is less restricted by seasonal or inter-annual flow variations (e.g. drought periods), and because it is much better protected from anthropogenic pollution. Due to increased temporal variability of surface water flows, climate change is likely to lead to higher demands for groundwater (Taylor *et al* 2013, Kundzewicz and Döll 2009). In some semi-arid and arid regions with intensive irrigation, abstraction rates exceeding groundwater recharge have resulted in strong groundwater depletion (Wada *et al* 2012). To support a sustainable groundwater management, it is necessary to assess renewable groundwater resources, i.e. long-term average annual groundwater recharge. Scenarios of future renewable groundwater resources under the impact of climate change can help to identify regions with significantly changing groundwater resources and thus inform planning of climate change adaptation measures.

Using global hydrological models, global groundwater recharge and thus renewable groundwater resources were estimated to be ∼13 000–15 000 $km^3$ $yr^{-1}$ under current climate conditions, and to account for approximately one third of the total renewable water resources (Döll and Fiedler 2008, Wada *et al* 2010). Döll (2009) assessed the impact of climate change on renewable groundwater resources as well as the related vulnerability based on four climate scenarios representing two emissions scenarios and two global climate models (GCM). These scenarios were used as input to the global hydrological model WaterGAP which computes groundwater recharge as a function of total runoff, precipitation intensity, relief, soil texture, aquifer properties and the occurrence of glaciers and permafrost. Due to the applied delta change approach, the study of Döll (2009) did not include the impact of increased future daily precipitation variability which is expected to lead to an overestimation of groundwater recharge in humid areas where infiltration capacity may be exceeded, and to an underestimation in semi-arid areas as the daily threshold precipitation, above which groundwater recharge occurs, is not exceeded often enough.

Here, we present results of a study of the impact of climate change on global renewable groundwater resources with WaterGAP that significantly extends the impact study of Döll (2009) with respect to the number and range of considered GHG emissions scenarios and the number of GCMs. In the study presented here, we take into account changes in future precipitation variability by applying bias-corrected daily climate model output (Hempel *et al* 2013) as developed within the Inter-Sectoral Impact Model Intercomparison Project (ISI-MIP, Warszawski *et al* 2013). For ISI-MIP, data from five GCMs from the CMIP5 archive (Taylor *et al* 2012, see table 1) were selected that cover four 'Representative Concentration Pathways' (RCPs) scenarios (Moss *et al* 2010) and the time period 1950–2099. The goal of the study is to clarify the benefits of avoided GHG emissions, i.e. low emissions pathways, with respect to renewable groundwater resources and groundwater recharge. While significant decreases of groundwater resources can be assumed to be detrimental under almost all circumstances, a significant increase may not always be beneficial. Rising groundwater tables may lead to flooding of basements or wetting of agricultural soils. As done in other ISI-MIP studies (Schewe *et al* 2013, Haddeland *et al* 2013), the possible positive impacts of climate mitigation are also analysed by relating GWR changes to the rise of global mean temperature (GMT) as predicted by the individual GCMs.

## 2. Data and methods

### *2.1. Input data*

*2.1.1. Climate data.* The World Climate Research Programme (WCRP), with its Working Group on Coupled Modelling in the fifth phase of the Coupled Model Intercomparison Project (CMIP5), had 20 GCM model groups involved to run their models for future conditions of greenhouse gas emissions, so-called RCPs. The different pathways (Moss *et al* 2010, their table 1) are named according to their radiative forcing in W $m^{-2}$ at the end of the 21st century as RCP2.6, RCP4.5, RCP6.0, to RCP8.5 (Taylor *et al* 2012, van Vuuren *et al* 2011, p 11).

Within ISI-MIP, five CMIP5 GCMs were selected, each of which providing climate projections until 2099 for the four RCPs: HadGEM2-ES, IPSL-CM5A-LR, MIROC-ESM-CHEM, GFDL-ESM2M, and NorESM1-M (table 1). GCM selection was primarily based on availability, at project start, of daily GCM data of the required variables for all RCPs for the period 1950–2099 (Hempel *et al* 2013). The selected models cover a broad response space defined by global temperature (figure 1(b)) and the ratio of land-averaged precipitation increase per GMT increase against GMT increase at the end of the 21st century with RCP8.5. The ratio ranges from approximately 0.3 to 1.0 (figure 3 in ISI-MIP 2013b). As GCM output differs significantly from observations, GCM output was bias-corrected before being used as input to impact models like WaterGAP. Bias-correction of daily temperature, precipitation, radiation and other variables was done using quantile mapping (Piani *et al* 2010, Hempel *et al* 2013).

**Table 1.** Global climate models selected for ISI-MIP.

| Global climate model | Institute acronym | Institute full name |
|---|---|---|
| HadGEM2-ES | MOHC (additional realizations by INPE) | Met Office Hadley Centre and Instituto Nacional de Pesquisas Espaciais |
| IPSL-CM5A-LR | IPSL | Institut Pierre-Simon Laplace |
| MIROC-ESM-CHEM | MIROC | Japan Agency for Marine-Earth Science and Technology, Atmosphere and Ocean Research Institute (The University of Tokyo), and National Institute for Environmental Studies |
| GFDL-ESM2M | NOAA GFDL | NOAA Geophysical Fluid Dynamics Laboratory |
| NorESM1-M | NCC | Norwegian Climate Centre |

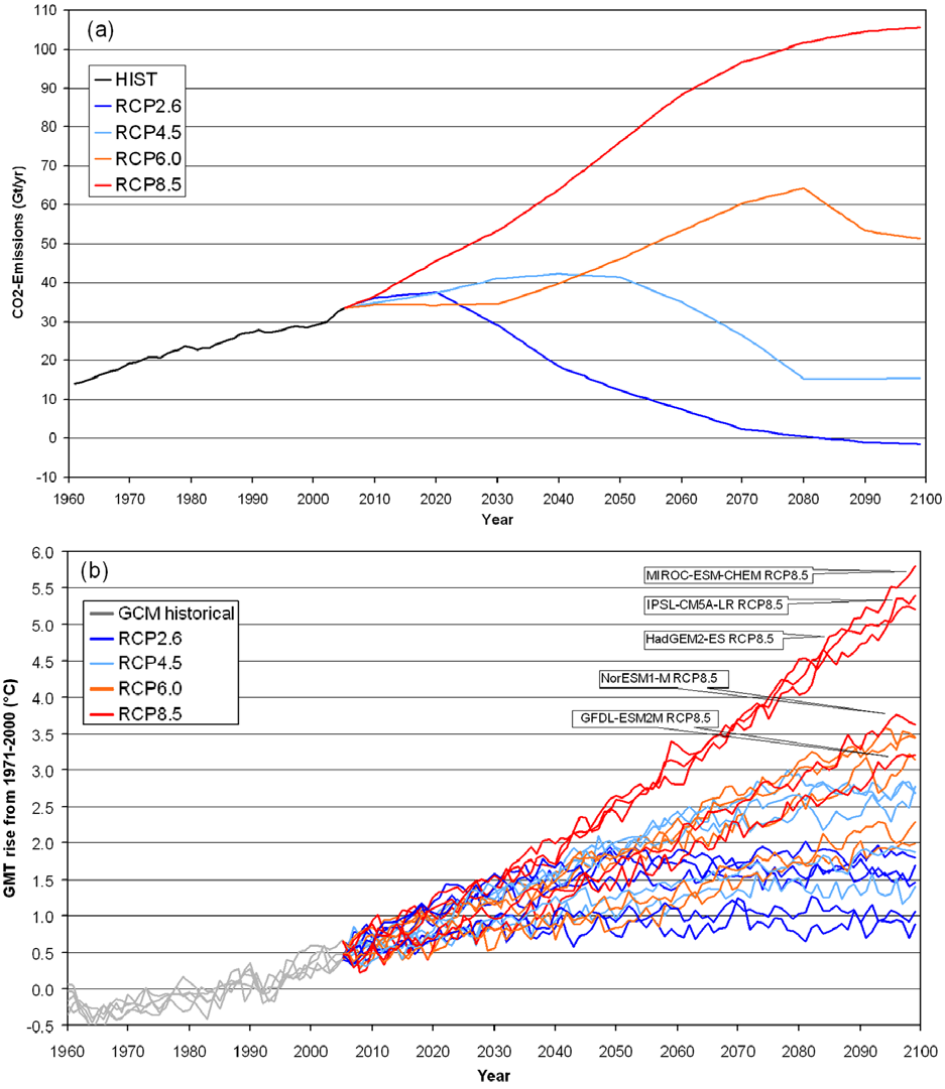


**Figure 1.** $CO_2$-emissions from anthropogenic and natural sources as a function of time (1961–2099) (a), global mean temperature (GMT, without bias-correction) as a function of time (1961–2099), as compared to 1971–2000 (add 0.4 °C as compared to pre-industrial conditions) (b), for historical periods until 2005, and starting in 2006 for RCPs 2.6, 4.5, 6.0, and 8.5, for five different GCMs, respectively.

GCM projections were simultaneously re-gridded to the 0.5° × 0.5° grid of the Climatic Research Unit of the University of East Anglia (CRU) and bias-corrected to the reference data set of WATCH Forcing Data (WFD) (Weedon *et al* 2011) for the period 1960–1999.

*2.1.2. Population data.* To assess the impact on population in the future, gridded population data were projected to the future period according to one selected Shared Socio-ecosystem Pathway (SSP), here the 'Middle of the Road' scenario SSP2 (ISI-MIP 2013a, SSP Database

2013, O'Neill 2012). The 0.5° × 0.5° gridded population data set was produced by scaling the 2010 GPWv3 gridded population dataset (available at http://sedac.ciesin.columbia.edu/data/collection/gpw-v3) with the SSP country totals (neglecting changes in population distribution within countries). The gridded population of the year 2085 was taken as representative for the end of the 21st century, summing to 9.886 billion individuals.

### *2.2. Modelling climate change impacts on renewable groundwater resources*

We used the global hydrological and water use model WaterGAP (Döll *et al* 2003, 2012, Flörke *et al* 2013) for simulating current and future water resources. WaterGAP computes runoff, groundwater recharge (GWR) as well as water use with a spatial resolution of 0.5° × 0.5° (55 km × 55 km at the equator) for all land areas except Antarctica. For this study, WaterGAP was run with the WATCH-CRU land mask and, using WFD climate input total runoff was calibrated against long-term average river discharge of 1971–2000 at more than 1200 gauging stations. All runs that applied bias-corrected GCM output were based on parameters of this calibration. Land use was standardized to follow Global Land Cover Characterization (GLCC) and CORINE (for Europe) using IGBP-classification.

GWR is determined by partitioning total runoff from land in each grid cell into GWR and fast surface and subsurface runoff. Partitioning of runoff takes into account soil texture, relief, hydrogeological conditions and the existence of glaciers and permafrost (Döll and Fiedler 2008). Only total runoff, but not groundwater recharge itself is calibrated, due to lack of observed data. GWR is assumed to be constrained by a maximum daily groundwater recharge rate, which is a function of soil texture. In semi-arid and arid areas, GWR is assumed to occur, in case of medium to coarse grained soils, only if daily precipitation exceeds 12.5 mm $d^{-1}$. This leads to an unbiased GWR estimation (Döll and Fiedler 2008, Tögl 2010). WaterGAP only simulates GWR from land (diffuse recharge via the soil) but neglects point recharge from surface water bodies. GWR estimates of WaterGAP have been judged to be plausible by experts in their regional domain within the WHYMAP Global Map of Groundwater Resources (Döll and Fiedler 2008).

Climate change impacts on future GWR were analysed using computed annual groundwater recharge from 1950 to 2099 (first years for spin-up) for all RCPs and GCMs. As absolute groundwater recharge estimates for historic time periods vary among model runs with WFD and the five different climate model outputs as input to WaterGAP, analyses focus on per cent changes of GWR. They were computed as the difference between GCM-specific future GWR and GWR during the reference period 1971–2000 as computed by the same GCM. Ensemble means are averages of the GCM-specific per cent changes.

Analyses reported here include the per cent changes of long-term average annual GWR from 1971–2000 until 2070–2099 (the 2080s), for each RCP. In addition, in line with the ISI-MIP Fast Track simulation protocol and evaluations (ISI-MIP 2013b, Warszawski *et al* 2013, e.g. Schewe *et al* 2013, Davie *et al* 2013), GWR changes as a function of GCM- and RCP-specific GMT were determined, following the approach of similar impact studies (Parry *et al* 2001, Tang and Lettenmaier 2012). Time slices were determined according to GMT rises with respect to pre-industrial GMT of 1.5–4 °C, in 0.5 °C increments, specifying 30 year average periods, e.g. 2004–2033 for 1.5 °C for RCP8.5 for HadGEM2-ES (Haddeland *et al* 2013). The time slices were defined for each GCM and extreme scenarios RCP2.6 and RCP8.5 from annual GMT anomalies from the 30 year reference period mean, using non bias-corrected time series including ocean cells. After adding 0.4 °C for GMT offset of the reference mean from pre-industrial conditions and averaging over running 30 year periods, the start and end of the periods were determined from the first occurrence of predefined GMT rises or as final maximum rise (Jens Heinke, pers. comm.). For final evaluation of up to six GCM–RCP-specific periods, annual GWR were averaged while GMT rises were rounded to standard values, e.g. for GFDL-ESM2M and RCP2.6 the maximum of 1.291 to 1.5 °C.

## 3. Results

### *3.1. Greenhouse gas emissions and global mean temperature rise*

The four applied emissions scenarios cover a broad range of possible futures, as illustrated in figure 1(a) by the development of the dominant $CO_2$ emissions (Meinshausen *et al* 2011). Cumulative 21st century emissions range from 1558 $GtCO_2$ (RCP2.6) to 7278 $GtCO_2$ (RCP8.5) (van Vuuren *et al* 2011, p 23). The five selected GCMs translate historical forcing to a GMT for the reference period 1971–2000 ranging from 12.8 to 14.2 °C, and GMT increases from the reference period 1971–2000 as projected by the GCMs for each RCP also differ appreciably (figure 1(b)). Over all 20 GCM runs, GMT increase ranges between ∼0.9 and ∼5.8 °C in 2099. The five GCMs fall into two groups from regarding GMT rise, with NorESM1-M and GFDL-ESM2M projecting much less GMT rise over time for each RCP. Averaged over the five GCMs, the very low emissions scenario RCP2.6 is projected to lead to an increase of 1.46 °C by 2099, while the very high emissions scenario RCP8.5 is projected to reach an increase of 4.9 °C as compared to 1971–2000. While there is a stabilization of GMT for RCP2.6 between 2040 and 2050 and for RCP4.5 after 2080, temperatures continue to rise for the higher emissions RCPs after 2099.

### *3.2. Global totals of groundwater recharge*

Long-term average annual GWR during 1971–2000 is simulated to be 13 404 $km^3$ $yr^{-1}$ when observed WFD is used as climate input. The GCMs, though bias-corrected against WFD, result in volumes between 13 633 $km^3$ $yr^{-1}$ (GFDL-ESM2M) and 14 450 $km^3$ $yr^{-1}$ (MIROC-ESM-CHEM). Therefore, to show the temporal development of global

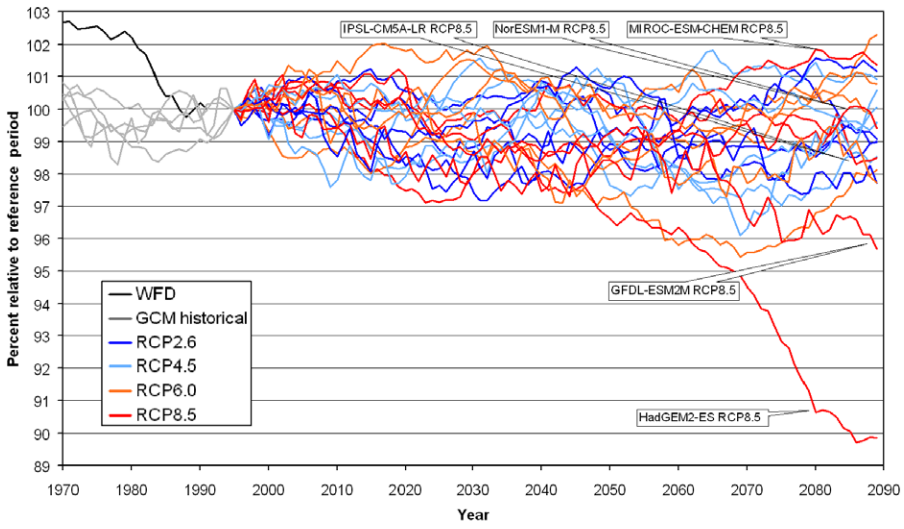


**Figure 2.** Temporal development of global groundwater recharge (running 20 year average, e.g. 1970 value represents average for 1961–1980) for each member of the ensemble (4 RCPs by 5 GCMs) as computed by WaterGAP. Global groundwater recharge as computed from observed climate data (WFD) is shown for comparison. GCM-based results are scaled to the GCM-specific reference value for the last historical 20 year period 1986–2005 which is set to 100%, as the RCP scenarios start in 2006. WFD-based results are scaled to period 1982–2001, as 2001 is the most recent year with available data.

totals of groundwater recharge as 20 year running averages (figure 2), the data were scaled to WFD- or GCM-specific averages of annual groundwater recharge during the last 20 years of historic time (1985–2004 for HadGEM2-ES, 1986–2005 for the other GCMs, 1982–2001 for WFD). For the historic time period, the WFD-derived 20 year averages of global groundwater recharge show a downward trend while GCM-derived values have no trend. This broadly follows the tendency in historic total precipitation over land (figure A.1) and historic global runoff (figure A.2). For the period 1971–2000, annual precipitation over land is between 111 918 $km^3$ $yr^{-1}$ (IPSL-CM5-AR) and 114 987 $km^3$ $yr^{-1}$ (NorESM1-M), being 111 543 $km^3$ $yr^{-1}$ for WFD, while annual runoff ranges between 43 600 $km^3$ $yr^{-1}$ (IPSL-CM5-AR) and 45 686 $km^3$ $yr^{-1}$ (GFDL-ESM2M), being 47 833 $km^3$ $yr^{-1}$ for WFD. Averaged over the five GCMs, global GWR decreases after 2050 for every RCP as compared to the specific reference period and also as compared to 1971–2000. The higher the emissions, the larger are the decrease and the spread among GCMs. While GWR predominantly decreases over all GCMs with values between 90% and 103% relative to the reference period (figure 2) at the end of the 21st century, both global precipitation over land and runoff increase to relative values of 99–111% (figure A.1) and 98–114% (figure A.2), respectively. This is a consequence of the applied soil-specific maximum daily groundwater recharge rate (section 2.2). Any daily runoff beyond this maximum recharge rate will only result in additional surface runoff. For RCP8.5, GWR decreases most strongly by around 10% with HadGEM2-ES (figure 2) that starts with second highest GWR total of 14 332 $km^3$ $yr^{-1}$ in 1971–2000. Most severe decreases until 2070–2099 are expected especially in regions with high GWR during 1971–2000 (figure 3(a)), i.e. Amazon basin, and in tropical South East Asia, e.g. Sumatra, Borneo, southern Vietnam, and southern New Guinea (figure 3(b)). HadGEM2-ES shows second lowest total precipitation increase over land (to 104% of reference period for RCP8.5, figure A.1), strong increase in global mean temperatures increasing evapotranspiration (figure 1(b)), and small increase in global runoff (to 104% for RCP8.5, second lowest) (figure A.2). GFDL-ESM2M-driven simulations result in the second strongest GWR decrease (RCP8.5 to 96% of reference period) and generally low future changes in precipitation and runoff oscillating around 100%, that only at the end of the 21st century slightly increase to 102% and 104%, respectively, except for RCP2.6 (99% and 98%, respectively). GFDL-ESM2M starts at the lowest global GWR total and experiences decreases in the same regions as HadGEM2-ES with less relative and absolute changes. IPSL-CM5A-LR, the GCM with the strongest increase of future precipitation (for RCP8.5 up to 111%, due to a strong precipitation increase over the Amazon basin, figure A.3(b)) and runoff (to 114%), results in a slight GWR decrease to approximately 98%.

### *3.3. Spatial patterns of long-term average groundwater recharge*

Spatial patterns of long-term average GWR, i.e. renewable groundwater resources, were evaluated for current and future conditions for the strongest RCP8.5 during the 2080s (figure 3) and for GMT rises of 2 °C and 3 °C (figure 4), respectively. The spatial distribution of the ensemble of GCM-derived GWR during the reference period 1971–2000 (figure 3(a)) was found to be rather similar to WFD-derived values (not shown) which are again rather similar to simulation results obtained with different data sets of observed climate and different model versions (Döll and Fiedler 2008, Tögl 2010). While the GCM ensemble shows lower GWR in the western USA, it computes higher GWR in tropical Africa.

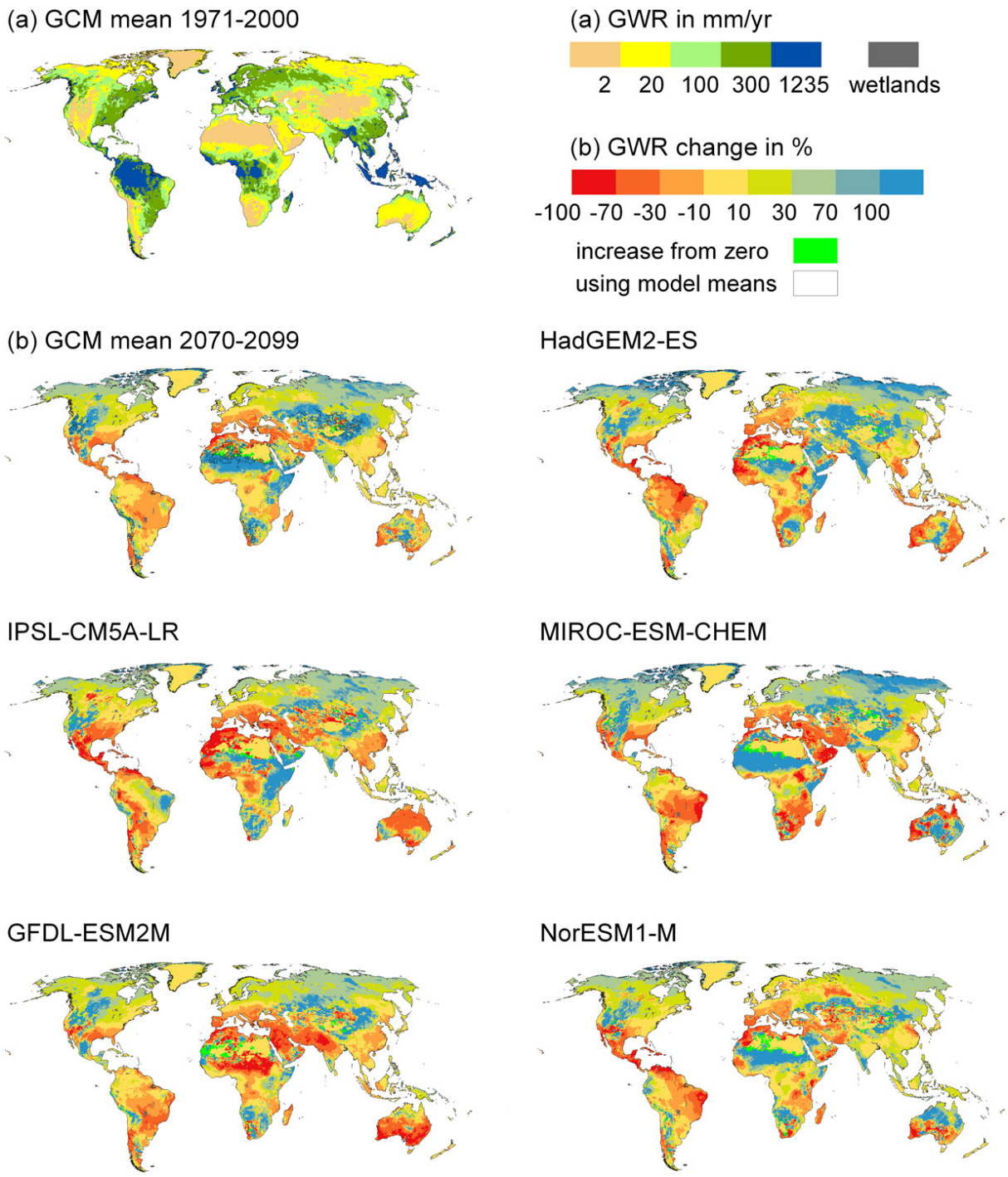


**Figure 3.** Groundwater recharge (GWR) as computed by WaterGAP for reference period 1971–2000 in mm $yr^{-1}$ for GCM ensemble mean (a), and projected per cent changes of GWR for the 2080s for RCP8.5, for five different GCMs and GCM ensemble mean (b). Black outlines in GCM ensemble mean changes show grid cells where at least one GCM increases from zero; there, we calculated the change by dividing the GCM mean of absolute GWR for the future by that for the reference period. Grey indicates grid cells with 100% wetlands where GWR is not calculated.

Per cent GWR changes until the 2080s range from decreases of more than 70% to increases of more than 100% compared to GWR during 1971–2000 (figure 3(b), classes represent changes classified as extreme (>70%), strong (30–70%), fair (10–30%), insignificant (<10%) change). According to all GCMs, a decrease of more than 10% is projected for large parts of South America, the Mediterranean, Mashriq, eastern China, southern Australia, central America, and southwestern South Africa. Significant increases are projected for northern latitudes, while some arid areas exhibit a possible increase of more than 100%. In large parts of the world, the individual GCMs have strongly differing patterns

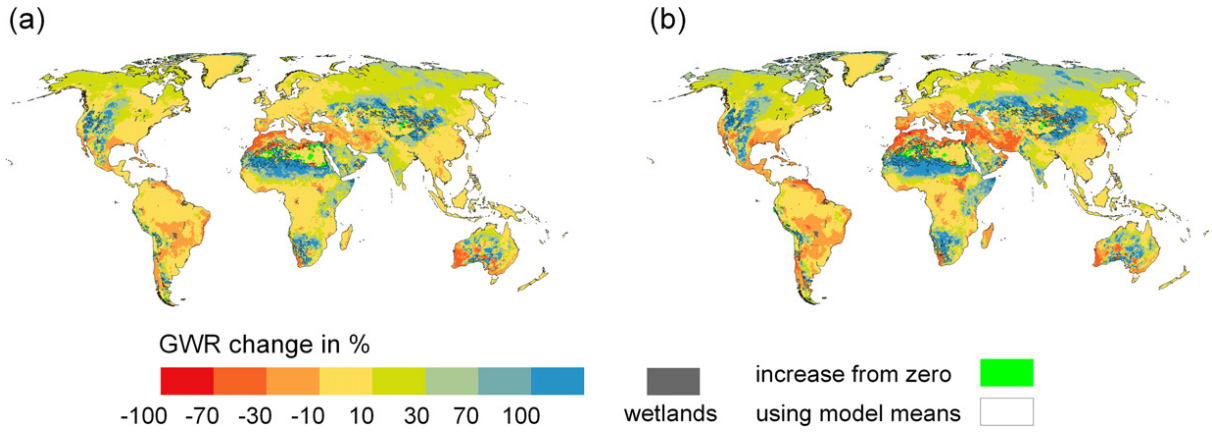


**Figure 4.** Projected per cent changes of groundwater recharge (GWR) as computed by WaterGAP for global mean temperature (GMT) rise of 2 °C (a) and 3 °C with respect to pre-industrial level (+0.4 °C for 1971–2000) (b) as mean over five different GCMs for RCP8.5. Black outlines show grid cells where at least one GCM increases from zero; there, we calculated the change by dividing the GCM mean of absolute GWR for the future by that for the reference period. Grey indicates grid cells with 100% wetlands where GWR is not calculated.

of change. An example is northern India, where groundwater resources are highly stressed. Depending on the GCM, a strong reduction of 30% or more, relatively stable GWR or GWR increases of more than 70% are projected. For northeastern Brazil, only two GCMs (MIROC-ESM-CHEM and NorESM1-M) show very strong decreases of GWR as also identified in Döll (2009) for the 2050s (emissions scenarios A2 and B2, ECHAM4 and HadCM3 GCMs). The decrease is less pronounced in the GCM ensemble mean as IPSL-CM5A-LR even projects a strong increase there. The strong decrease of GWR in the Amazon for HadGEM2-ES explains the strong decline of global GWR of RCP8.5 shown in figure 2. In general, GWR changes derived from HadGEM2-ES have a broad similarity with the GCM ensemble mean.

Generally, per cent GWR changes have the same sign as per cent precipitation changes (figure 3(b)), for RCP8.5. However, per cent GWR changes are much higher than per cent precipitation changes, which show a more homogeneous spatial pattern (figure A.3(b)). When absolute GWR for the reference period is low, the direction of change can differ between precipitation and GWR. Small absolute precipitation changes induce small absolute changes in GWR (e.g. less than +2 mm), which translate into comparatively big relative changes (e.g. up to +2800%), either positive or negative depending on the highly variable absolute value for the reference period. The limitation of groundwater recharge by a maximum daily groundwater recharge rate (section 2.2) is also visible, e.g. for a site in northern Kenya, where a mean increase in precipitation by 111% translates to a mean GWR increase of 60%, in the midst of stronger GWR per cent increases above 100% following precipitation increases of less than 100% (figures 3(b) and A.3(b)).

### *3.4. Groundwater recharge changes as a function of rise in global mean temperature*

Figure 4 shows that GWR changes intensify when GMT rise as compared to pre-industrial conditions increases from 2 to 3 °C. The spatial pattern of areas with GWR increases and decreases remains the same. We also analysed the influence of GMT rise on the land area that is subject to GWR decreases of more than 70%, 30% or 10%, and significant changes of more than ±10% (figure 5).

The area affected by different degrees of GWR changes increases with GMT rise. For a GMT rise of 2 °C compared to pre-industrial conditions, an ensemble mean of 2.0% (range 1.1–2.6%) of global land area is projected to suffer from an extreme decrease of renewable groundwater resources of more than 70%, while the affected areas increase to 3.0% (1.5–5.3%) and to 3.4% (1.9–4.8%) for a GMT rise of 3 °C and 4 °C, respectively. Note that for RCP8.5 only four models reach 3.5 °C GMT rise, and only three 4 °C (figure 5).

For extreme GWR decreases and for strong decreases larger than 30%, the increase in global land surface per degree of GMT rise is linear until 3 °C. For extreme changes, ∼1% land area is affected additionally per 1 °C (e.g. from 2 to 3 °C); for strong changes it is ∼4% (figures 5(a) and (b)). For more than 10% decrease, already at a GMT rise of 1.5 °C about 20% land surface is affected (figure 5(c)); while for any change of more than 10% this figure is ∼55%, i.e. ∼35% of the land area is subject to a GWR increase (figure 5(d)). When global warming increases from 2 to 3 °C, an additional 5% land area is projected to be affected by a GWR decrease of more than 10% (figure 5(c)), while at the same time an additional 5% are subject to a GWR increase of more than 10% (figure 5(d)).

When evaluating GWR changes as a function of GMT rise, there are only small differences between RCP8.5 and RCP2.6, as can be seen for GMT rise of 1.5 °C with respect to the pre-industrial conditions (i.e. +1.1 °C from reference period) (figure 5). Other ISI-MIP analyses (e.g. Schewe *et al* 2013) compared all four RCPs and found only small differences of impacts at a certain GMT rise derived from various RCPs.

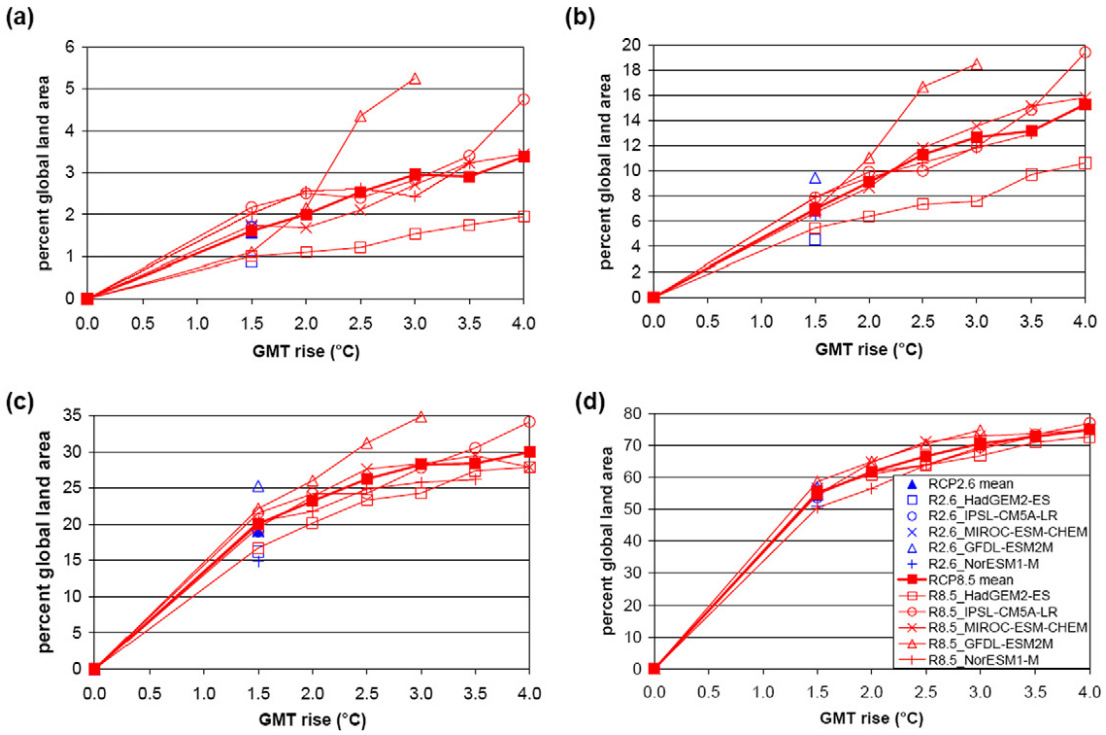


**Figure 5.** Per cent of global land area (except Greenland and Antarctica) subject to projected changes of groundwater recharge (as computed by WaterGAP) as a function of global mean temperature rise as compared to pre-industrial conditions (+0.4 °C for 1971–2000). Results are derived from RCP8.5 runs of five GCMs, and classified for changes of more than −70% (GWR > 70% decrease) (a), more than −30% (GWR > 30% decrease) (b), more than −10% (GWR > 10% decrease) (c), more than ±10% (GWR > 10% change) (d); the difference (d) − (c) specifies per cent of land area with more than 10% GWR increase.

**Table 2.** Per cent of land area ('Area', excluding Greenland and Antarctica) and population ('Pop', in 2085) affected by changes in groundwater recharge between 1971–2000 and 2070–2099, as computed by WaterGAP applying four climate change scenarios (RCP 2.6, 4.5, 6.0, and 8.5) from five GCMs. In each field, average, minimum and maximum from all models are given. Cells with zero groundwater recharge in the reference period, but more in the future fall into a separate class. The last row with decreases of more than 10% is an aggregation of the first three classes.

| GWR change class (%) | RCP2.6 | | RCP4.5 | | RCP6.0 | | RCP8.5 | |
|---|---|---|---|---|---|---|---|---|
| | Area | Pop | Area | Pop | Area | Pop | Area | Pop |
| −100 to −70 | 1.7 (0.9–2.7) | 0.9 (0.5–1.9) | 2.3 (1.7–2.8) | 1.2 (0.9–1.5) | 2.6 (1.2–3.7) | 1.6 (0.7–2.5) | 4.2 (2.7–5.3) | 4.3 (2.1–8.3) |
| −70 to −30 | 6.6 (3.7–9.5) | 6.4 (1.7–14.1) | 7.8 (6.5–9.6) | 8.3 (4.8–11.5) | 9.1 (5.4–11.7) | 10.4 (5.2–15.0) | 13.1 (9.6–15.6) | 14.7 (9.1–17.5) |
| −30 to −10 | 13.0 (8.0–15.6) | 16.5 (8.6–23.6) | 13.6 (12.1–14.7) | 16.7 (13.2–18.8) | 14.8 (11.7–17.5) | 19.6 (12.2–28.4) | 14.1 (11.5–16.2) | 19 (14.1–24.5) |
| −10–10 | 38.4 (29.2–47.3) | 46.8 (39.5–57.4) | 32.6 (26.8–36.6) | 41.5 (37.9–49.6) | 29.5 (25.5–34.9) | 36.5 (33–44.6) | 22.0 (19.7–25.2) | 28.6 (24–36.1) |
| 10–30 | 20.2 (17.1–22.4) | 14.4 (9.4–18) | 19.8 (17.1–21.8) | 15.4 (11.3–20.3) | 18.2 (14.9–21.7) | 12.9 (10.6–16.0) | 14.5 (12.2–18.0) | 12.5 (8.8–16.3) |
| 30–70 | 9.6 (7.3–13.6) | 7.9 (2.8–13.0) | 11.5 (8.3–15.2) | 8.9 (4.5–12.3) | 12.2 (10.3–14.6) | 8.7 (4.9–12.2) | 15.0 (14.0–16.5) | 9.4 (7.2–11.6) |
| >70 | 9.4 (7.0–11.6) | 7 (2.0–12.2) | 11.2 (8.5–15.5) | 7.8 (2.5–12.8) | 12.6 (8.3–17.3) | 10.1 (2.4–15.5) | 15.9 (10.2–20.9) | 11.5 (4.1–16.5) |
| Increase from zero | 1.2 (0.7–1.6) | 0.2 (0.1–0.5) | 1.2 (0.8–1.7) | 0.2 (0.1–0.3) | 1.1 (0.8–1.5) | 0.2 (0.1–0.4) | 1.2 (0.9–1.6) | 0.1 (0.1–0.1) |
| Less than −10% | 21.3 (14.6–27.2) | 23.8 (10.8–38.5) | 23.7 (21.5–26.8) | 26.2 (22.6–31.9) | 24.6 (18.3–31.6) | 31.6 (18.1–45.3) | 31.3 (26.3–35.1) | 37.9 (26.6–50.2) |

### *3.5. Population and land areas affected by groundwater recharge changes*

For the end of the 21st century, we analysed the influence of RCPs across GCMs on both per cent of population and per cent of land area that are subject to certain GWR changes (table 2). The affected population is assumed to be equal to the population within a grid cell that is concerned. The percentage of global population (SSP2 population scenario) suffering from a decrease of renewable groundwater resources of more than 10% by the 2080s as compared to 1971–2000 increases from 24% (range 11–39%) for RCP2.6 to 26% (23–32%) for RCP4.5, 32% (18–45%) for RCP6.0, and 38% (27–50%) for RCP8.5 (table 2). The respective average percentages of land areas are smaller, i.e. 21% (15–27%) for RCP2.6, 24% (22–27%) for RCP4.5, 25% (18–32%) for RCP6.0, and 31% (26–35%) for RCP8.5, respectively. If emissions could be reduced from RCP8.5 to RCP2.6, the population that is projected to be spared from a significant change of GWR would increase from 29% to 47% of the global population. When comparing affected land areas to affected population, it is obvious that areas with decreasing and constant renewable groundwater resources are those with a relatively high population density (except those suffering a decrease of more than 70%), while it is mostly the less densely populated areas of the Arctic, the Sahara and Central Asia that are projected to experience increased groundwater resources.

## 4. Discussion

### *4.1. Bias-corrected climate input*

Climate scenarios calculated by GCMs are subject to significant uncertainties in particular regarding precipitation (Covey *et al* 2003). Therefore, for historic time periods, GCM precipitation differs strongly from observations and, as a consequence, original GCM scenario output cannot be used directly as input to hydrological models if reasonable values of runoff and groundwater recharge are required (Kundzewicz *et al* 2007, Hagemann *et al* 2011). Direct use of precipitation and potential evapotranspiration data computed by GCMs for historic time periods produces biases in simulated mean monthly river flows (Prudhomme and Davies 2009) and other hydrological output. Therefore, in the climate change impact study of Döll (2009), like in many other impact studies, the delta change method was applied to combine climate change information produced by GCMs with (interpolated) observational data of historic climate. In this method, climate input for a future time period is computed by considering differences (in case of temperature) or ratios (in case of precipitation) between long-term average monthly GCM data for future and current time periods. These are then added to or multiplied with observed monthly time series to obtain future time slices that can be used to determine changes in long-term averages of hydrological variables like groundwater recharge. Disadvantages of this method are that transient climate changes cannot be represented and that changes in inter-annual or daily climate variability are not taken into account. Using GCM output that is bias-corrected against observational data of historic climate is an alternative way of combining GCM data with observational data that overcomes these drawbacks (Hempel *et al* 2013, Hagemann *et al* 2011, Piani *et al* 2010). However, while use of daily GCM data with monthly bias-correction was shown to reduce the bias of simulated runoff as compared to observed historic runoff, bias-correction significantly altered the climate change signal of precipitation and temperature for specific locations and months (Hagemann *et al* 2011). Hagemann *et al* (2011, p 575) concluded that 'for some regions, the impact of the bias-correction on the climate change signal may be larger than the signal itself, thereby identifying another level of uncertainty that is comparable in magnitude to the uncertainty related to the choice of the GCM…'. In our study, we found that bias-corrected GCM input results in global GWR without any temporal trend during the second half of the 20th century, whereas when the observational data set that was used for bias-correction is applied as input to WaterGAP, there is a clear decreasing trend. This could be caused by the bias-correction method when lower values of precipitation are increased, while higher values are decreased through correction.

### *4.2. Multi-GCM analysis*

In a previous study on estimating future GWR (Döll 2009) only two GCMs were used. The current analysis of five GCMs showed that a bigger GCM ensemble enlarges the estimated uncertainty range for groundwater recharge projections. Using all of the CMIP5 GCMs would probably further increase the range, but this was not possible with the given data availability and resources in time and personal. However, the selection procedure of the GCMs ensured a broad coverage of impacts from temperature and precipitation increase. Given the well-known large uncertainties of climate models, it is important to show, in impact analysis, the uncertainties stemming from climate models (and other steps of the modelling chain), such that identification of adaptation measures to climate change is done without a false sense of certainty about future climate change.

In case of multi-GCM analysis, presentation of ensemble means, in particular in maps, is popular due to its conciseness and the assumed increased robustness of mean changes where the errors of individual models are balanced (Milly *et al* 2005). However, presenting only multi-GCM means of climate change impacts is misleading. In particular, the range of projected changes of e.g. GWR is reduced due to the averaging, which may lead to an underestimation of the risks of climate change. If, for example, in the case of only two GCMs, one model projects a decrease of −20% and the other an increase of 10%, the multi-GCM mean shown would be −5%. Presenting some agreement of variability measures can help (Schewe *et al* 2013), but are difficult to show in maps and hard to understand by non-experts. Therefore, we strongly feel that presentation of GCM-specific patterns of change in maps like in figure 3 is very helpful for understanding uncertainty of the spatial patterns of change.

### *4.3. Impacts as a function of global mean temperature rise*

Plotting of per cent of global land area affected by certain changes of impact variable (figure 5) against GMT rise follows the approach of Parry *et al* (2001) who used only one GCM across four emissions scenarios. Tang and Lettenmaier (2012) showed runoff changes as a function of GMT, across 23 GCMs and three emissions scenarios, where (like in our case, see figure 5) not much dependency on the choice of the emissions scenario was visible.

Concerning functional relationships between GWR change and GMT rise, we found two different relationships. We found sigmoidal functions, which were identified for water shortage by Parry *et al* (2001) and for discharge by Schewe *et al* (2013), if we computed the land area suffering from relatively small per cent changes of GWR of more than $\pm 10\%$. There, the affected area strongly increases between 0 and 1.5 °C GMT rise but then levels off. In contrast, we found a rather linear relationship for stronger GWR decreases of more than 30% or even 70%. As the sigmoidal shape of the area affected by small impacts may lead to the wrong impression that the benefits of climate change mitigation decrease strongly beyond a GMT rise of 1.5 °C, it is important to also quantify the area affected by stronger GMT increases, where the linear shape indicates that e.g. preventing an increase of GMT rise from 2 to 3 °C has approximately the same benefits as preventing an increase from 1 to 2 °C.

Presenting climate change impacts as a function of GMT rise only, without any specific indication of time, is problematic when climate change impacts are quantified not only as changes of the physical system but are related to population (Schewe *et al* 2013) or population-related measures like water use. In different climate models and under different emissions scenarios, a certain GMT rise is reached at different points in time (see figure 1); it is impossible to transparently and meaningfully express e.g. a climate change impact at a certain GMT as, for example, a fraction of global population affected, if the population existing at the point in time when the GMT is reached is used. In each model and RCP, the impact value that is shown at any one GMT relates to different population values and patterns which are not shown in the graphs. Parry *et al* (2001) related GMT to population at a specified time, and the steepness of the sigmoidal water shortage curve for 2080 resulted from newly included huge city populations in India and China. Hence, plots like figure 5 would be difficult to interpret if affected population instead of affected area were used. Relating affected population at a certain point in time as a function of specific emissions scenarios, like we did in table 2, appears to be a more transparent way of presenting the benefits of avoided emissions and global warming.

### *4.4. People affected by changes in groundwater recharge*

For various reasons, we assumed that all people living in a grid cell are directly or indirectly affected by GWR changes in this grid cell. Groundwater globally contributes to 36% for domestic, 27% for manufacturing, and 42% for irrigation sector water withdrawals (Döll *et al* 2012), and typically is withdrawn within the same grid cell where it is used. Thus, only a fraction of the people living in a grid cell is directly affected by GWR changes, as their source of freshwater supply is groundwater. But all inhabitants of a grid cell are indirectly affected. If, for example, GWR decreases, groundwater is becoming locally less available, and additional surface water resources must be used, such that decreases in GWR also affect surface water users which are very likely to suffer from concurrent decreases of surface water availability due to climate change. Subsequent economic effects of decreased groundwater availability may be increased costs for water delivery. Increasing GWR, on the other hand, affects people e.g. by a rise in groundwater table above critical levels that possibly causes damage to basements of public or private buildings and infrastructure, or wetting of agricultural soils which then require artificial drainage.

### *4.5. Further uncertainties*

There are a number of further uncertainties that affect the outcome of our study. These include the method for computing changes in potential evapotranspiration PET due to climate change, the effect of land use change on GWR, and how the impact of climate change and $CO_2$ increase on vegetation will affect GWR. In addition, we shortly discuss the influence of neglecting GWR from surface water bodies and the relevance of our results for areas with groundwater depletion.

In WaterGAP, PET is modelled as a function of net radiation and temperature using the Priestley–Taylor approach. In this study, however, we did not analyse directly the impact of changes in net radiation, but only the impact of temperature changes when analysing results as a function of GMT rise, e.g. in figures 4 or 5. Besides, different $\alpha$ factors for humid (1.26) and arid (1.74) climate conditions are applied in WaterGAP following Shuttleworth (1993). The latter value corresponds well to theoretical maximum values derived for high saturation deficits at stations in semi-arid regions, and leads to relatively higher PET estimates which are closer to those calculated by the well-parameterized Penman–Monteith method (McAneney and Itier 1996). However, due to climate change, the boundaries of regions classified as humid and arid will change (Kingston *et al* 2009), and this fact was not taken into account in this study. Though, in semi-arid and arid regions where decreases of groundwater recharge are most problematic, actual evapotranspiration from soil is mostly limited by available soil water and not PET.

Land use change like conversion to agricultural land or irrigated agriculture can have significant impacts on GWR. We computed only GWR from precipitation and not from irrigation return flow, and thus also did not take into account the possible climate change induced alterations of irrigation water use on GWR at the grid cell level which can be important when irrigation water withdrawals are high (Döll *et al* 2012). Increased $CO_2$-concentrations may lead

to an increased water use efficiency (biomass production per transpired water volume, so-called physiological effect) and thus decreased transpiration, but also increased biomass production (so-called structural effect), which may balance the physiological effect. In addition, climate change itself may lead to vegetation change. It may either lead to higher or lower biomass production, leaf area index and rooting depths, affecting transpiration and thus runoff (Murray *et al* 2012) and GWR (McCallum *et al* 2010). These complex and highly uncertain processes are simulated by dynamic vegetation models but not hydrological models. While the net effect of the dynamic vegetation are highly model-dependent, there appears to be the tendency that consideration of dynamic vegetation may lead, in most world regions, to overall decreased transpiration estimates as compared to static vegetation (Murray *et al* 2012, Wiltshire *et al* 2013). Therefore, WaterGAP possibly overestimates future decreases of groundwater recharge.

The projected GWR decreases in semi-arid regions do not consider potential contributions of focused recharge from surface water bodies including ephemeral streams which are known to be significant in semi-arid regions. If we simulated GWR from surface water bodies, projected GWR decreases might be somewhat lower. Possibly, however, GWR from surface water bodies would also decrease in areas of decreased runoff due to decreased water table elevations and areas of surface water bodies. In addition to that, there are areas where groundwater is currently depleted by water abstractions exceeding GWR. To what extent groundwater depletion (e.g. in India, China, USA, and Arabian countries, see Foster and Loucks 2006) will be affected by projected changes of GWR depends on the ratio of GWR over net groundwater abstractions (Döll *et al* 2012). Only where the ratio is very small, e.g. in Saudi-Arabia, depletion will not be affected by the GWR changes assessed in this letter.

## 5. Conclusions

In this study, the impact of four future GHG emissions pathways on global renewable groundwater resources was assessed. The uncertainty of climate model projections was taken into account by applying a small ensemble of five bias-corrected GCMs, using daily input data for the period 1950–2099.

A novel approach to look at climate change impacts for groundwater recharge representing renewable groundwater resources as a function of GMT rises across different GCM–RCP ensemble members was applied. Sigmoidal functions found in other studies for, e.g. water shortage and discharge, exist here only for per cent of global land area affected by GWR decreases larger than 10% decrease or any significant changes greater than ±10%. In contrast, the per cent of global land area that is affected by GWR decreases of more than 30% and 70% increases linearly with global warming from 0 to 3 °C. For each degree of GMT rise, an additional 4% of the global land area is affected by a GWR decrease of more than 30%, and an additional 1% is affected by a decrease of more than 70%.

Looking at a selected time slices instead of GMT rises makes it possible to quantify, in a transparent way, the population that will be affected by climate change impacts under different emissions pathways, and to thus determine the benefits of avoided emissions. The percentage of projected global population suffering from a significant decrease of GWR of more than 10% by the 2080s as compared to the reference period 1971–2000 decreases from 38% in the high emissions scenario RCP8.5 to 24% in the low emissions scenario RCP2.6. If we could achieve emissions according to RCP2.6, 47% of the population would be spared from any significant GWR change increases, instead of only 29% in the case of RCP8.5. Increases of GWR are more likely to occur in areas with below average population density, while GWR decreases of more than 30% affect especially (semi)arid regions, across all GCMs.

Both approaches for analysing climate change impacts show how much mankind would benefit from avoided emissions. The large uncertainty of projected impacts of GHG emissions due to GCM uncertainty does not prevent us from clearly identifying the benefits of emissions reductions regarding GWR. However, we expect that the uncertainty range would become larger if more GCMs and more than one global hydrological model were applied (comp. Schewe *et al* 2013), and if the alteration of transpiration due to the impact of climate change and $CO_2$ increases on vegetation were simulated. Then, it might be more difficult to ascertain the GWR-related benefits of GHG emissions reductions.

## Acknowledgments

This work has been conducted under the framework of ISI-MIP. The ISI-MIP Fast Track project was funded by the German Federal Ministry of Education and Research (BMBF) with project funding reference number 01LS1201A. Responsibility for the content of this publication lies with the authors. We acknowledge the World Climate Research Programme's Working Group on Coupled Modelling, which is responsible for CMIP, and we thank the respective climate modelling groups (listed in table 1) for producing and making available their model output. For CMIP the US Department of Energy's Program for Climate Model Diagnosis and Intercomparison provides coordinating support and led development of software infrastructure in partnership with the Global Organization for Earth System Science Portals. The Hessian state supported the work within the LOEWE initiative funding of the Biodiversity and Climate Research Centre (BiK-F). We thank Jens Heinke (PIK) for specifying years for GMT rise, Felipe Colón González and Adrian Tompkins (ICTP) for projected gridded population data, and Malte Meinshausen (PIK) for time series of greenhouse gas emissions. We thank the two anonymous reviewers who helped us to improve the quality and clarity of our letter.

## Appendix

(See figures A.1–A.3).

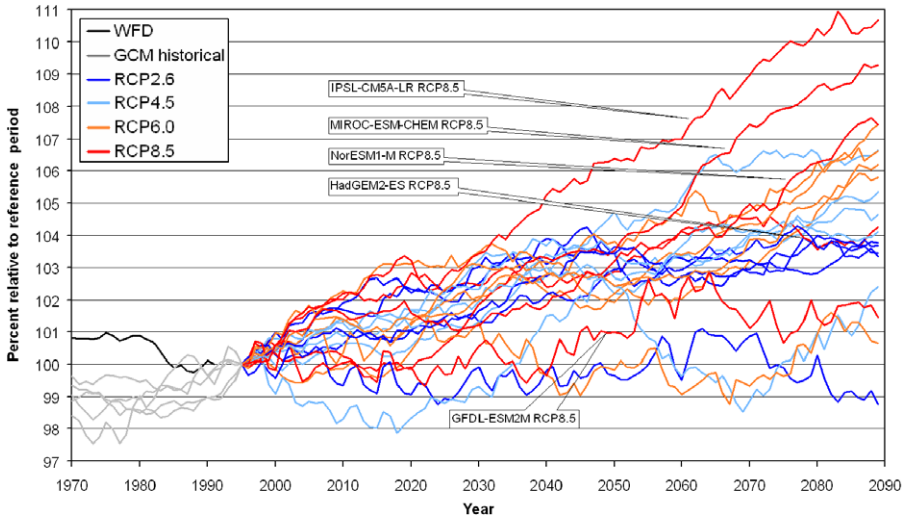


**Figure A.1.** Temporal development of total precipitation over land (running 20 year average of bias-corrected data, e.g. 1970 value represents average for 1961–1980) for each member of the ensemble (4 RCPs by 5 GCMs). Observed climate data (WFD) are shown for comparison. GCM-based results are scaled to the GCM-specific reference value for the last historical 20 year period 1986–2005 which is set to 100%, as the RCP scenarios start in 2006. WFD-based results are scaled to period 1982–2001, as 2001 is the most recent year with available data.

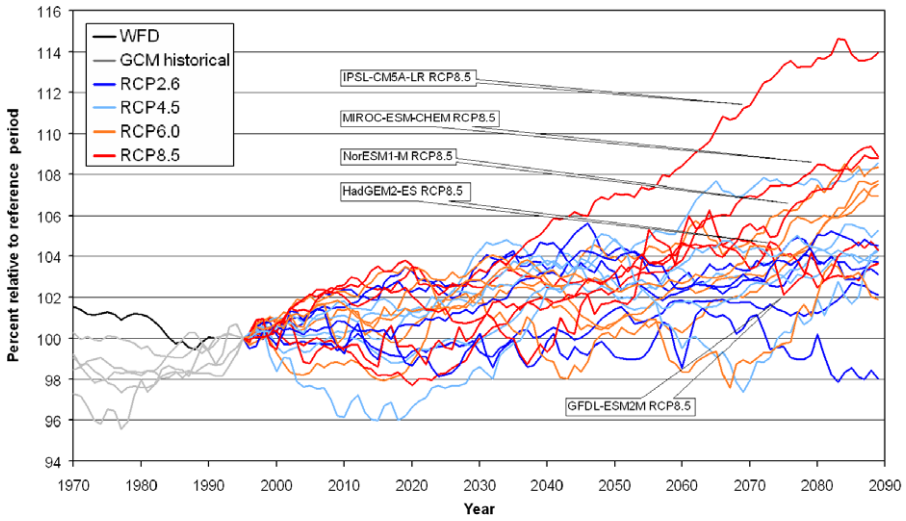


**Figure A.2.** Temporal development of global runoff (running 20 year average from bias-corrected input data, e.g. 1970 value represents average for 1961–1980) for each member of the ensemble (4 RCPs by 5 GCMs). Global runoff as computed from observed climate data (WFD) is shown for comparison. Here, we used the same scaling as for precipitation in figure A.1.

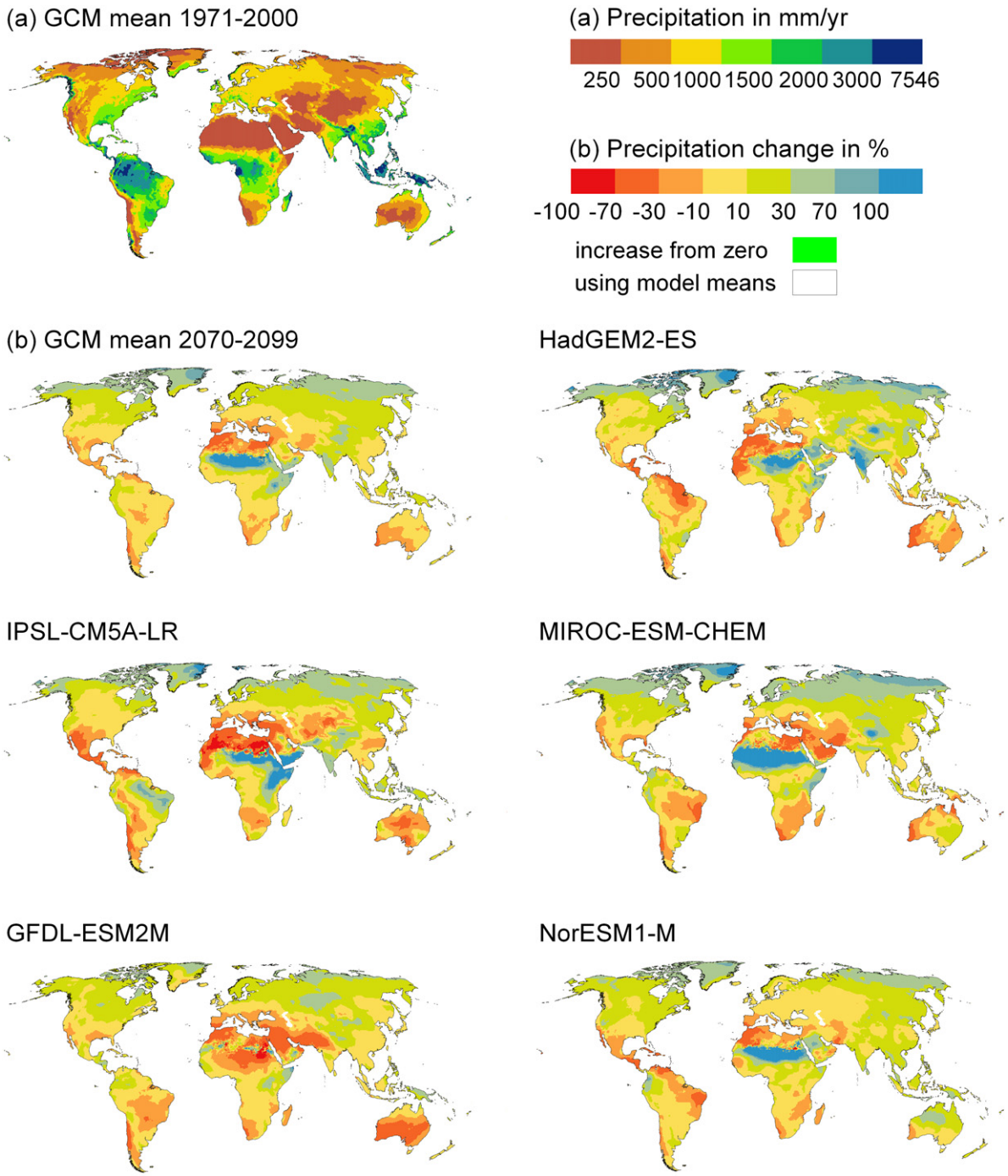


**Figure A.3.** Precipitation for reference period 1971–2000 in mm $yr^{-1}$ for GCM ensemble mean (a), and projected per cent changes of precipitation for the 2080s for RCP8.5, for five different GCMs and GCM ensemble mean (b). Black outlines in GCM ensemble mean changes show nine grid cells in Egypt and Sudan where at least one GCM increases from zero; there, we calculated the change by dividing the GCM mean of absolute precipitation for the future by that for the reference period.

## References


Covey C, Achuta Rao K M, Cubasch U, Jones P, Lambert S J, Mann M E, Phillips T J and Taylor K E 2003 An overview of results from the coupled model intercomparison project *Glob. Planet. Change* **37** 103–33

Davie J C S *et al* 2013 Comparing projections of future changes in runoff and water resources from hydrological and ecosystem models in ISI-MIP *Earth Syst. Dyn. Discuss.* **4** 279–315

Döll P 2009 Vulnerability to the impact of climate change on renewable groundwater resources: a global-scale assessment *Environ. Res. Lett.* **4** 036006

Döll P and Fiedler K 2008 Global-scale modeling of groundwater recharge *Hydrol. Earth Syst. Sci.* **12** 863–85

Döll P, Hoffmann-Dobrev H, Portmann F T, Siebert S, Eicker A, Rodell M, Strassberg G and Scanlon B R 2012 Impact of water withdrawals from groundwater and surface water on continental water storage variations *J. Geodyn.* **59/60** 143–56

Döll P, Kaspar F and Lehner B 2003 A global hydrological model for deriving water availability indicators: model tuning and validation *J. Hydrol.* **270** 105–34

Flörke M, Kynast E, Bärlund I, Eisner S, Wimmer F and Alcamo J 2013 Domestic and industrial water uses of the past 60 years as a mirror of socio-economic development: a global simulation study *Glob. Environ. Change* **23** 144–56

Foster S and Loucks D P (ed) 2006 *Non-Renewable Groundwater Resources: A Guidebook on Socially-Sustainable Management for Water-Policy Makers* (*UNESCO IHP-VI Series on Groundwater* vol 10) (Paris: United Nations Educational, Scientific and Cultural Organization) (http://unesdoc.unesco.org/images/0014/001469/146997E.pdf)

Haddeland I *et al* 2013 Global water resources affected by human interventions and climate change *Proc. Natl Acad. Sci.* in review

Hagemann S, Chen C, Haerter J O, Heinke J, Gerten D and Piani C 2011 Impact of a statistical bias correction on the projected hydrological changes obtained from three GCMs and two hydrology models *J. Hydrometeorol.* **12** 556–78

Hempel S, Frieler K, Warszawski L, Schewe J and Piontek F 2013 A trend-preserving bias correction—the ISI-MIP approach *Earth Syst. Dyn. Discuss.* **4** 49–92

ISI-MIP 2013a *SSP Data of the Inter-Sectoral Impact Model Intercomparison Project (ISI-MIP)* (www.pik-potsdam.de/research/climate-impacts-and-vulnerabilities/research/rd2-cross-cutting-activities/isi-mip/input-data/ssp-data, last accessed: 6 May 2013)

ISI-MIP 2013b *Simulation Protocol of the Inter-Sectoral Impact Model Intercomparison Project (ISI-MIP)* (www.pik-potsdam.de/research/climate-impacts-and-vulnerabilities/research/rd2-cross-cutting-activities/isi-mip/simulation-protocol/isi-mip_simulationprotocol-as-of-05-november-2012-website, last accessed: 6 May 2013)

Kingston D G, Todd M C, Taylor R G, Thompson J R and Arnell N W 2009 Uncertainty in the estimation of potential evapotranspiration under climate change *Geophys. Res. Lett.* **36** L20403

Kundzewicz Z W and Döll P 2009 Will groundwater ease freshwater stress under climate change? *Hydrol. Sci. J.* **54** 665–75

Kundzewicz Z W, Mata L J, Arnell N W, Döll P, Kabat P, Jiménez B, Miller K A, Oki T, Sen Z and Shiklomanov I A 2007 Freshwater resources and their management *Climate Change 2007: Impacts, Adaptation and Vulnerability. Contribution of Working Group II to the Fourth Assessment Report of the Intergovernmental Panel on Climate Change* ed M L Parry, O F Canziani, J P Palutikof, P J van der Linden and C E Hanson (Cambridge: Cambridge University Press) pp 173–210 (www.ipcc.ch/publications_and_data/ar4/wg2/en/ch3.html)

McAneney K J and Itier B 1996 Operational limits to the Priestley–Taylor formula *Irrig. Sci.* **17** 37–43

McCallum J L, Crosbie R S, Walker G R and Dawes W R 2010 Impacts of climate change on groundwater in Australia: a sensitivity analysis of recharge *Hydrogeol. J.* **18** 1625–38

Meinshausen M *et al* 2011 The RCP greenhouse gas concentrations and their extension from 1765 to 2300 *Clim. Change* **109** 213–41

Milly P C D, Dunne K A and Vecchia A V 2005 Global pattern of trends in streamflow and water availability in a changing climate *Nature* **438** 347–50

Moss R H *et al* 2010 The next generation of scenarios for climate change research and assessment *Nature* **463** 747–56

Murray S J, Foster P N and Prentice I C 2012 Future global water resources with respect to climate change and water withdrawals as estimated by a dynamic global vegetation model *J. Hydrol.* **448** 14–29

O'Neill B 2012 Workshop on the nature and use of new socioeconomic pathways for climate change research *Meeting Report Final Version (Boulder, CO, November, 2011)* p 37 (www.isp.ucar.edu/sites/default/files/Boulder%20Workshop%20Report_0.pdf)

Parry M, Arnell N W, McMichael T, Nicholls R, Martens P, Kovats S, Livermore M, Rosenzweig C, Iglesias A and Fischer G 2001 Millions at risk: defining critical climate change threats and targets *Glob. Environ. Change* **11** 181–3

Piani C, Weedon G P, Best M, Gomes S M, Viterbo P, Hagemann S and Haerter J O 2010 Statistical bias correction of global simulated daily precipitation and temperature for the application of hydrological models *J. Hydrol.* **395** 199–215

Prudhomme C and Davies H 2009 Assessing uncertainties in climate change impact analyses on the river flow regimes in the UK. Part 1: baseline climate *Clim. Change* **93** 177–95

Schewe J *et al* 2013 Multi-model assessment of water scarcity under climate change *Proc. Natl Acad. Sci.* in review

Shuttleworth W J 1993 Evaporation *Handbook of Hydrology* ed D R Maidment (New York: McGraw-Hill) pp 4.1–4.53

Siebert S, Burke J, Faures J M, Frenken K, Hoogeveen J, Döll P and Portmann F T 2010 Groundwater use for irrigation—a global inventory *Hydrol. Earth Syst. Sci.* **14** 1863–80

SSP Database 2013 *SSP Database Version 0.9.3* (available at https://secure.iiasa.ac.at/web-apps/ene/SspDb, last accessed: 6 May 2013)

Tang Q and Lettenmaier D P 2012 21st century runoff sensitivities of major global river basins *Geophys. Res. Lett.* **39** L06403

Taylor K E, Stouffer R J and Meehl G A 2012 An overview of CMIP5 and the experiment design *Bull. Am. Meteorol. Soc.* **93** 485–98

Taylor R G *et al* 2013 Ground water and climate change *Nature Clim. Change* **3** 322–9

Tögl A C 2010 Global groundwater recharge: evaluation of modeled results on the basis of independent estimates *Bachelor Thesis* Johann Wolfgang Goethe-University Frankfurt am Main, Frankfurt am Main, Institute of Physical Geography

van Vuuren D P *et al* 2011 The representative concentration pathways: an overview *Clim. Change* **109** 5–31

Wada Y, van Beek L P H, Sperna Weiland F C, Chao B F, Wu Y H and Bierkens M F P 2012 Past and future contribution of global groundwater depletion to sea-level rise *Geophys. Res. Lett.* **39** L09402

Wada Y, van Beek L P H, van Kempen C M, Reckman J W T M, Vasak S and Bierkens M F P 2010 Global depletion of groundwater resources *Geophys. Res. Lett.* **37** L20402

Warszawski L, Frieler K, Piontek F, Schewe J, Serdeczny O and Huber V 2013 Research design of the intersectoral impact model intercomparison project (ISI-MIP) (in preparation)

Weedon G P, Gomes S, Viterbo P, Shuttleworth W J, Blyth E, Österle H, Adam J C, Bellouin N, Boucher O and Best M 2011 Creation of the WATCH forcing data and its use to assess global and regional reference crop evaporation over land during the twentieth century *J. Hydrometeorol.* **12** 823–48

Wiltshire R B A, Betts R, Booth B, Dennis E, Falloon P, Gornall J and McNeall D 2013 The relative importance of population, climate change and $CO_2$ plant physiological forcing in determining future global water stress *Glob. Environ. Change* submitted